Nucleic Acids Research, 1992, Vol. 20, No. 24 6723–6732

The effect of loop size in antisense and target RNAs on the efficiency of antisense RNA control

Tord Hjalt and E.Gerhart H.Wagner
Department of Microbiology, Biomedical Center, Uppsala University, Box 581, S-751 23 Uppsala, Sweden

Received July 13, 1992; Revised and Accepted September 24, 1992

ABSTRACT

Most natural antisense RNAs display a high degree of secondary structure with stem-loops as their most prominent feature. Mutations affecting the inhibitory activity of these RNAs most often map in or close to loop regions in both the antisense and target RNAs. The primary recognition loops often contain 5–7 unpaired nucleotides. Nucleotide changes in the loops affect the binding rate and, hence, the inhibitory effect on the activity of the target RNA. Here we address the question whether loop sizes affect binding rates between antisense and target RNAs, using the replication control system of plasmid R1 as a model system. By creating a series of loop size mutants we show that loop size alterations have strong effects on the binding rates between the two reactant RNAs *in vitro*, and that most of the mutations analyzed display corresponding effects on antisense RNA control *in vivo*. Our data suggest that the three-dimensional structures of antisense and target RNA stem-loops are crucial for determining binding rates. The implications of these results for the design of efficient artificial antisense RNA control systems are discussed.

INTRODUCTION

Antisense RNAs have been identified as very specific and efficient inhibitors of gene expression in a variety of prokaryotic systems, and have more recently also been reported to occur in eukaryotes (1, 2, 3). These RNAs are most often small, ranging in size from ≈70–120 nt (1). Usually, antisense and target RNAs are transcribed from the same DNA segment, but in opposite directions, such that both RNAs are completely complementary.

The most detailed studies related to antisense RNA control have been performed on two bacterial plasmids, R1 and ColE1 (4, 5), in which antisense RNAs function as copy number control elements, and on the transposon Tn*10*, where translation of transposase mRNA is inhibited by an antisense RNA (1). In all three systems, *in vitro* binding between the antisense and target RNAs has been characterized. In particular, the details of the binding pathways and the kinetics of the binding reactions have been extensively studied for CopA/CopT (antisense and target RNAs of plasmid R1 [6, 7, 8]) and for RNAI/RNAII (antisense and target RNAs of ColE1-type plasmids [9, 10, 11]). These *in vitro* studies indicated that the binding rate constants measured for antisense-target RNA pairs are similar, in the order of 10^6 $M^{-1}s^{-1}$.

Both CopA/CopT and RNAI/RNAII binding proceeds in at least two experimentally distinguishable steps: formation of a transient 'kissing complex' formed between complementary loop nucleotides, followed by a subsequent nucleation step that initiates complete RNA duplex formation. This second step requires complementary, single-stranded regions distal to the stem-loop(s) where the primary binding occurs. The requirement for single-stranded regions outside the stem-loops is due to the topological constraints which do not permit helix propagation starting from two interacting loops (7). The analyses of the ColE1 and R1 systems showed that the rate-limiting step in the binding pathway is the formation of a kissing complex, and that overall binding is kinetically irreversible (8, 11).

A common denominator for efficient antisense RNAs is their high degree of secondary structure. The above-mentioned RNAs consist of one (RNA-OUT of Tn*10*), two (CopA of plasmid R1) or three stem-loops (RNAI of ColE1-type plasmids) and some additional single-stranded regions. The sites of primary interactions between antisense and target RNAs have been identified through mutational analysis, and, generally, mutations altering certain loop nucleotides result in altered inhibitory properties and new specificities (4, 12, 13). The loops involved in the primary recognition event most often consist of 5–7 unpaired nucleotides. Internal loops and bulged-out nucleotides are often found close to the loops; the significance of this observation is so far unclear.

We have previously investigated the replication control circuit of plasmid R1 in detail. The antisense RNA, CopA, is the main copy number control element of this plasmid (4). It is constitutively transcribed and is turned over rapidly *in vivo*. This implies that the concentration of CopA RNA in the cell represents a measure of the copy number of the plasmid. CopA, by binding to its target, the leader region of the RepA mRNA (CopT), inhibits the synthesis of the replication rate-limiting RepA protein (see Figure 1B). We have recently demonstrated that RepA synthesis requires the translation of a short leader peptide reading frame, *tap*, which is located in the intergenic region between the *copA* gene and the *repA* reading frame. *RepA* is translationally coupled to *tap* and, thus, CopA inhibits *repA* expression indirectly by inhibition of *tap* translation (14).

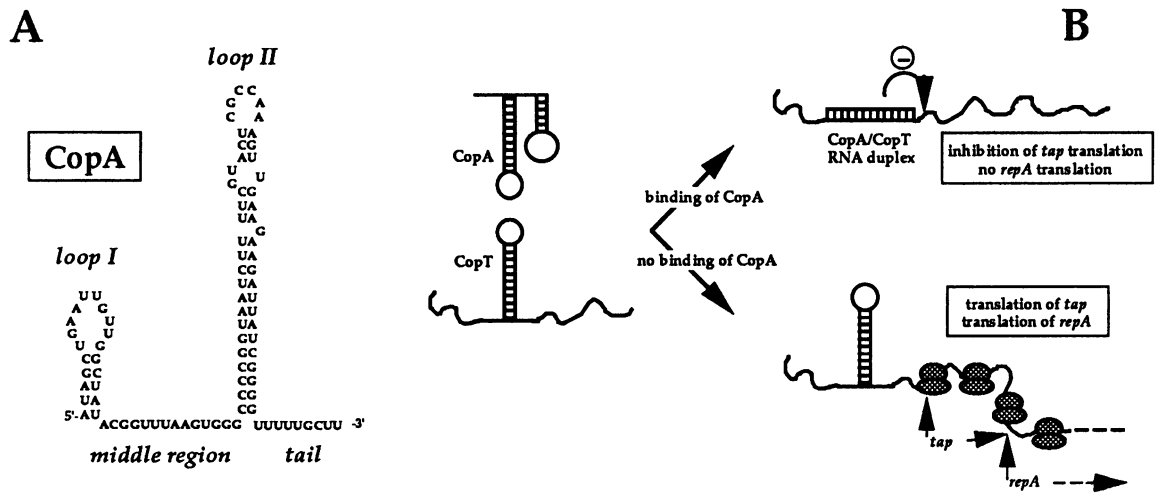

Figure 1. A) The secondary structure of CopA RNA. The structure of wild-type CopA RNA is shown (16). The loop regions I and II, the middle region and the 3′−tail are indicated. **B)** A simplified model for CopA-mediated inhibition of RepA synthesis. The Figure indicates schematically the branched pathway, by which the synthesis of the replication rate-limiting RepA protein is controlled. Binding of CopA to CopT inhibits translation of *tap* and, indirectly, of *repA*. Failure of CopA to bind to CopT permits translation of the *tap* reading frame and, by translational coupling, of *repA* [for details, see (14)].

A variety of R1 mutants with altered plasmid copy numbers and incompatibility properties have been identified previously (see 4, 15). Most of these mutants carry base changes in the DNA sequences coding for the major loop II of CopA and CopT (see Figure 1A). This is consistent with the conclusion that loop II is the main determinant for the overall binding rate between the two RNAs. However, two previously characterized copy number up-mutants (see 15, and references therein), suggest that factors other than the primary loop sequences may affect binding. These mutations alter the size of loop II, resulting in smaller (plasmid pKN104) or larger loops (plasmid pKN102) (16). In particular, the mutation in pKN102 is not located within any of the six normal loop nucleotides, but in the upper part of the stem, which results in an opening of this structure to form a ≈15 nt loop. This observation might suggest that the structure of the loops is important for proper recognition, and that small or large loops can mediate adverse effects on the rate-limiting step of the binding pathway.

We now report results of a systematic analysis of loop size effects using the CopA/CopT system of plasmid R1 as a model. This system is feasible for such an analysis, since 1) binding of the antisense RNA, CopA, to its target, CopT, initiates at only one major loop, 2) the *in vitro* binding properties of CopA and CopT have been well characterized previously, and 3) assays for the *in vivo* effect of the antisense RNA are available. A series of CopA/CopT RNA pairs, in which the wild-type 5′-CGCCAA-3′/3′-GCGGUU-5′ loop II sequence was replaced by C_nAA/G_nUU, was tested for binding rates *in vitro*. The effect of the mutations *in vivo* was assessed by measuring *repA-lacZ* expression and by determining relative plasmid copy numbers. Our data indicate that, using the particular sequences tested here, 5−7 nucleotides in the CopA loop II results in maximal binding rates *in vitro*. The *in vivo* results support this conclusion, although for the largest loops, abberant behaviour was observed when *repA* expression and copy numbers were assayed.

Based on these results, we suggest that appropriate presentation of a small number of nucleotides in a highly ordered three-dimensional structure is favorable for rapid formation of the 'kissing intermediate', and thus, for rapid RNA duplex formation. The relevance of these findings is discussed with regard to strategies for developing efficient artificial antisense RNA control systems.

MATERIALS AND METHODS

Bacterial strains and plasmids

The *Escherichia coli* strain MC1061 [*araD139*, (*Δara-leu)7697*, *lacZ74*, *galU*, *hsdR*, *rpsL*] (17) was used as a host for plasmid constructions and for the *repA-lacZ* fusion plasmid experiments. The *E.coli* strain KL16*polA* [λ⁻, relA1, spoT1, thi-1, PO45, *polA*::Tn*10*] was used for plasmid copy number determinations of the the R1-pMB1-hybrid plasmids described below. This strain is non-permissive for replication of the pMB1-part of the chimaeric plasmids used below, but permissive for replication of the R1 replicon. The *E.coli* strain NM522 [*supE*, *thi*, *hsd5*, *Δ(lac-proAB)*, F′/*proA*⁺*B*⁺, *lacI*^{q}*ZM15*/], harboring plasmid pGW58 (18) was used for the synthesis of single-stranded (+) strand plasmid DNA for site-directed mutagenesis.

The plasmids, their construction, and their origin is summarized in Table 1. Plasmid pGW58 is a derivative of pMa5-8 which carries a 0.65 kbp segment of R1 DNA. The R1 segment contains the regulatory *copA-copT* region and ends within the *repA* gene (18). The mutant derivatives of pGW58, pGW58-2C through pGW58-8C, were constructed by oligo-directed mutagenesis (see below). Plasmid pGW58-10 carries a *copA* promoter down-mutation and has been described previously (18).

The *repA-lacZ* translational fusion plasmid pGW177 has been described previously (14). It carries the fusion fragment on a p15A vector and confers resistance to kanamycin. Mutant derivatives pGW177-2C-L through pGW177-8C-L were constructed by replacing the R1-fragments between the unique *BglII* and *SalI* restriction sites of pGW177-L (wild-type fusion) by the corresponding fragments of the mutated pGW58-derivatives.

The pMB1-R1 hybrid plasmids were constructed as follows: We used the polymerase chain reaction (PCR) to amplify a 958 bp segment of plasmid pOU71 (19) with a set of primers, THBeco

Table 1. Plasmids

Plasmids	Description	Parent plasmid(s)	Source/Reference
pGW58	Cloned R1 control region, −296−+596[a](Δ*Bgl*II-*Bgl*II, *copB*⁻)	pMa5-8 + pJL133	(18)
pGW58-10	like pGW58, *copA* promoter down-mutation	pGW58 + pKN417	(18)
pGW58-2C	like pGW58, loop II mutation CGCC[b]→CC	pGW58	this work
pGW58-3C	like pGW58, loop II mutation CGCC→CCC	pGW58	this work
pGW58-4C	like pGW58, loop II mutation CGCC→CCCC	pGW58	this work
pGW58-5C	like pGW58, loop II mutation CGCC→CCCCC	pGW58	this work
pGW58-6C	like pGW58, loop II mutation CGCC→CCCCCC	pGW58	this work
pGW58-8C	like pGW58, loop II mutation CGCC→CCCCCCCC	pGW58	this work
pGW177-L	*repA-lacZ* translational fusion in p15A vector	pACYC177 + pGW58-L	(14)
pGW177-2C-L	like pGW177-L, loop II mutation CGCC→CC	pGW177-L + pGW58-2C	this work
pGW177-3C-L	like pGW177-L, loop II mutation CGCC→CCC	pGW177-L + pGW58-3C	this work
pGW177-4C-L	like pGW177-L, loop II mutation CGCC→CCCC	pGW177-L + pGW58-4C	this work
pGW177-5C-L	like pGW177-L, loop II mutation CGCC→CCCCC	pGW177-L + pGW58-5C	this work
pGW177-6C-L	like pGW177-L, loop II mutation CGCC→CCCCCC	pGW177-L + pGW58-6C	this work
pGW177-8C-L	like pGW177-L, loop II mutation CGCC→CCCCCCCC	pGW177-L + pGW58-8C	this work
pGW641	pMB1-R1 hybrid plasmid (Δ*Bgl*II-*Bgl*II, *copB*⁻)	pSP64 + pKN271	(20)
pGW64	pMB1-R1 hybrid plasmid (*copB*⁺)	pGW641 + pOU71	this work
pGW64-2C	like pGW64, loop II mutation CGCC→CC	pGW641 + pGW58-2C	this work
pGW64-3C	like pGW64, loop II mutation CGCC→CCC	pGW641 + pGW58-3C	this work
pGW64-4C	like pGW64, loop II mutation CGCC→CCCC	pGW641 + pGW58-4C	this work
pGW64-5C	like pGW64, loop II mutation CGCC→CCCCC	pGW641 + pGW58-5C	this work
pGW64-6C	like pGW64, loop II mutation CGCC→CCCCCC	pGW641 + pGW58-6C	this work
pGW64-8C	like pGW64, loop II mutation CGCC→CCCCCCCC	pGW641 + pGW58-8C	this work
pOU71	Temp.-amplifyable R1 replicon, λ/cI[857] control	pKN1562 + pBR322 + EDλ4::Tn*3*	(19)

[a] The numbers refer to nucleotide positions in (37).
[b] Letters refer to the nucleotides starting at the 5'-side of CopA loop II (see Figure 1). The complementary sequence of CopT is not shown.

and GW11 (see below). These primers were synthesized such that the former results in a change of the *Bgl*II-site located in front of the *copB* gene to an *Eco*RI-site, and the latter one spans the unique *Sal*I-site within the *repA* gene. After cleavage with the restriction enzymes *Eco*RI and *Sal*I, the isolated DNA-fragment was inserted into plasmid pGW641 (20) cleaved by the same enzymes. This procedure resulted in a pMB1-R1 chimaera, pGW41, which contains a wild-type R1 part and differs from the parent plasmid pGW641 by containing the intact *copB* gene with its promoter. In addition, the conversion of the proximal *Bgl*II-site to an *Eco*RI-site facilitated the use of the second *Bgl*II-site (located within the *copB* gene) for the construction of mutant derivatives. The mutant plasmids pGW41-2C through pGW41-8C were built by replacing the wild-type *Bgl*II-*Sal*I-fragment of pGW41 by the *Bgl*II-*Sal*I-fragments of mutant plasmids pGW58-2C to pGW58-8C.

Cell growth and media

Cells were grown in LB medium or on LA plates, made as described (21). When appropriate, antibiotics were included at 50 μg/ml.

Enzymes and chemicals

The enzymes and chemicals used were of the highest purity available. Enzymes were purchased from IBI or Kabi-Pharmacia unless otherwise stated. Radiochemicals were purchased from DuPont NEN.

DNA manipulations

Construction of plasmids, transformations and plasmid preparations were essentially according to (21).

Oligo-directed mutagenesis

Oligo-directed mutagenesis of the loop II region of *copA/copT* was done as described previously (22, 23). We used S-dCTP phosphorothioate analogs in second-strand synthesis, and the restriction enzyme *Ban*II for nicking of the parental (+) strand of pGW58. The deoxyoligoribonucleotides used were Mut2C-Mut8C (see below). Isolated plasmid DNA was sequenced by the dideoxy chain termination method (see below) to confirm the mutations created.

Sequencing of mutant plasmid DNA

Sequencing of plasmid DNA was done using Sequenase, according to a protocol supplied by the vendor (United States Biochemical Corporation).

Oligodeoxyribonucleotides

Mutagenic primers and primers for PCR were sythesized using a Pharmacia Gene Assembler Plus (Kabi-Pharmacia). The oligodeoxyribonucleotides used in this study had the following sequences (5'→3' direction): THBeco: AACAC AGAAT TCCGT CACAA TTCTC CAAGT CG; GW11: CGCCA GTCCT CACTA AATGG CCAGT GTGGT GAT; mutagenic oligos for creating *copA/copT* loop II mutation, Mut2C-Mut8C: TTTTC GTACT C_nAAAG TTGAA (where n= 2, 3, 4, 5, 6, or 8); primers for synthesizing CopA transcription templates containing a T7 promoter sequence were: T7AS (GAAAT TAATA CGACT CACTA TAGTA GCTGA ATTGT TGGCT ATACG) and T7AE (AAAGC AAAAA CCCCG ATAAT CTTC); primers for synthesizing CopT transcription templates containing a T7 promoter sequence were: T7-GG (GAAAT TAATA CGACT CACTA TAGGT TAAGG AATTT TGTGG CTGG) and T7T-E1 (CGTTT GGTGA AGATC AGTCA CACC); probes for Northern analyses: COP (TAATC TTCTT CAACT) and ProbeA (TAAAT CCACG TCAGA ACCA).

Determinations of relative plasmid copy numbers

Relative plasmid copy numbers were determined as described (24) by measuring the single-cell benzylpenicillin resistance level of KL16*polA* cells containing wild-type and mutant plasmids of

the pGW41-series. The *polA*-mutation in the host strain ensures that only the copy number of the R1-replicon of the pMB1-R1-hybrid is assayed.

β-galactosidase assay

The β-galactosidase assay used to measure synthesis of RepA-LacZ fusion protein *in vivo* was performed as described (25).

Northern blotting analyseis

Northern blotting analysis of CopA and CopT RNAs was performed as described (18). [^{32}P]-end-labelled oligodeoxyribonucleotides COP and ProbeA (see above) were used to probe for CopA and CopT RNA, respectively.

Synthesis of DNA templates for in vitro transcription of CopA and CopT RNAs

We used suitable pairs of primers (see below) to synthesize PCR-fragments from wild-type or mutant plasmids of the pGW58-series. The primer pairs were chosen so that the resulting CopA and CopT templates contained T7 RNA polymerase promoter sequences followed by CopA or CopT sequences, respectively. CopA RNA synthesized from such a template carries a G instead of an A residue as its 5′-terminal nucleotide. This change was introduced to facilitate transcription by T7 polymerase (26), and did not affect binding rates (data not shown). Similarly, CopT RNA carries two consecutive G's at the 5′-end instead of GU which is present in the authentic RepA mRNA. Transcription of CopT yields a run-off product of 273 nt. A 100 μl PCR reaction mixture contained: 10 mM Tris-HCl pH 8.3, 50 mM KCl, 1.5 mM $MgCl_2$, 200 μM dNTPs, ≈2 ng of plasmid DNA, 2.5 units of Taq DNA polymerase (Perkin-Elmer) and 0.5 μM of each of the two primers. The PCR reactions were run for 25 cycles in a Perkin-Elmer Cetus DNA Thermal Cycler (temperatures were 94°, 55° and 72°C for the denaturation, annealing and polymerization steps, respectively, with a 1 minute step time). Subsequently, the DNA-fragments were eluted after electrophoresis on a 2% agarose gel using a Mermaid kit (Bio 101, New England BioLabs), and frozen in 30 μl TE buffer (10 mM Tris-HCl pH 7.9, 1 mM Na_2EDTA).

Synthesis and isolation of CopA and CopT RNAs

Wild-type and mutant CopA RNA was transcibed *in vitro* from a PCR-fragment template (see above) using T7 RNA polymerase (Kabi Pharmacia). Incubation mixtures for uniformly labelled CopA contained in 100 μl: 40 mM Tris-HCl, pH 7.5, 6 mM $MgCl_2$, 11 mM DTT, 2 mM spermidine-Cl, 0.01% Triton X-100, 0.5 mM each of CTP, GTP, and ATP, 0.03 mM UTP, 25 μCi [α-^{32}P]UTP (DuPont NEN, 800 Ci/mmol), 40 units of RNAGuard (Kabi Pharmacia), 180 units of T7 RNA polymerase (Kabi Pharmacia) and ≈0.5 μg of template DNA. Incubations were at 37°C for four hrs. Two units of RQ1 DNase (Promega Biotech) was added, and incubation was continued for ten more minutes. The RNA was gel-purified and quantitated as described previously (6). CopT RNA was transcribed using the same protocol, but substituting [^{3}H]UTP (10 μCi in 100 μl) for [α-^{32}P]UTP, and increasing the final concentrations of all rNTPs to 0.5 mM. The specific actitivities of the purified CopT RNAs were calculated as described (6). The RNAs were finally dissolved in a suitable volume of TMN buffer [20 mM Tris-OAc pH7.5, 10 mM $Mg(OAc)_2$, 100 mM NaCl]. The RNAs were renatured by heating to 80°C, followed by slow cooling to 35°C. CopA and CopT RNAs were stored at −20°C.

CopA RNA for ribonuclease mapping was transcribed essentially as above, but the incubation was allowed to proceed overnight. In addition, the rNTP concentrations were raised to 4 mM each, 24 mM $MgCl_2$ was used, and ≈100 units of T7 RNA polymerase was included. The synthesized RNA was, after Sephadex G-50 chromatography, dephosphorylated using calf intestinal phosphatase, phenol-extracted, precipitated, and subsequently 5′-end-labelled with [γ-^{32}P]ATP and T4 polyribonucleotide kinase. The labelled RNAs were gel-purified and extracted as described above.

CopT RNA for ribonuclease mapping was obtained essentially as above. The 5′-end-label was introduced during transcription by including 2 μl (20 μCi) of [γ-^{32}P]GTP. Consequently, the GTP concentration was decreased to 0.04 mM, and UTP was raised to 0.5 mM.

CopA RNA/CopT RNA binding rate determinations

Binding experiments were carried out as in (6). A more than ten-fold molar excess of [^{3}H]-labelled CopT was incubated with [^{32}P]-labelled CopA in TMN buffer at 37°C. Samples were withdrawn at different time points, and the reaction was stopped by the addition of 1.4 volumes of FD (92% formamide, 17 mM Na_2EDTA, 0.05% xylene cyanol, 0.05% bromophenol blue, 0.4% SDS) on ice. The final concentrations of [^{3}H]CopT RNAs ranged between 1×10^{-9} M and 3×10^{-8} M.

Band intensities on the dried gels used for the binding experiment were quantitated using a Molecular Dynamics PhosphorImager 400S (Molecular Dynamics). The apparent second order binding rate constants (k_{app}) were calculated from the slopes of lin-log plots of the percentage of unbound CopA versus time, as described in (6).

Ribonuclease mapping of the loops II of CopA and CopT RNAs

Partial RNase T2 digests of CopA transcripts were performed in TMN buffer essentially as described (16). The reaction volume was 5 μl. In the experiment shown in Figure 2A, 0.04 units of RNase T2 (Sigma) was used for ≈0.09 pmoles of CopA RNA. Carrier tRNA was present at ≈0.08 μg/μl. The reaction mixtures were incubated at 37°C for 5 minutes, and then stopped by pipetting into tubes containing 450 μl of water, 10 μg of carrier tRNA and 500 μl of phenol/chloroform. After three extractions, the RNA was precipitated, centrifuged, dried, and subsequently dissolved in 5 μl water. After adding 5 μl of FD, the samples were boiled and electrophoresed on 8% sequencing gels, followed by autoradiography on Kodak X-Omat AR film.

The protocol for secondary structure mapping of CopT RNAs was identical, except that 0.004 units of ribonuclease T1 was employed.

RESULTS

Structures of CopA and CopT RNAs of the loop-size mutants

A series of loop size mutations was introduced into the *copA/copT* sequence of plasmid pGW58 by oligo-directed mutagenesis (Materials and Methods). To minimize primary sequence effects in the functional assays for CopA/CopT interactions, we first altered the wild-type loop II sequence of CopA from 5′-CGCC-AA-3′ to 5′-CCCCAA-3′, resulting in the corresponding change to 3′-GGGGUU-5′ in the target RNA, CopT (mutation in pGW58-4C, Table 1). Subsequently, we created a series of mutants with 2, 3, 4, 5, 6, and 8 consecutive C residues in loop

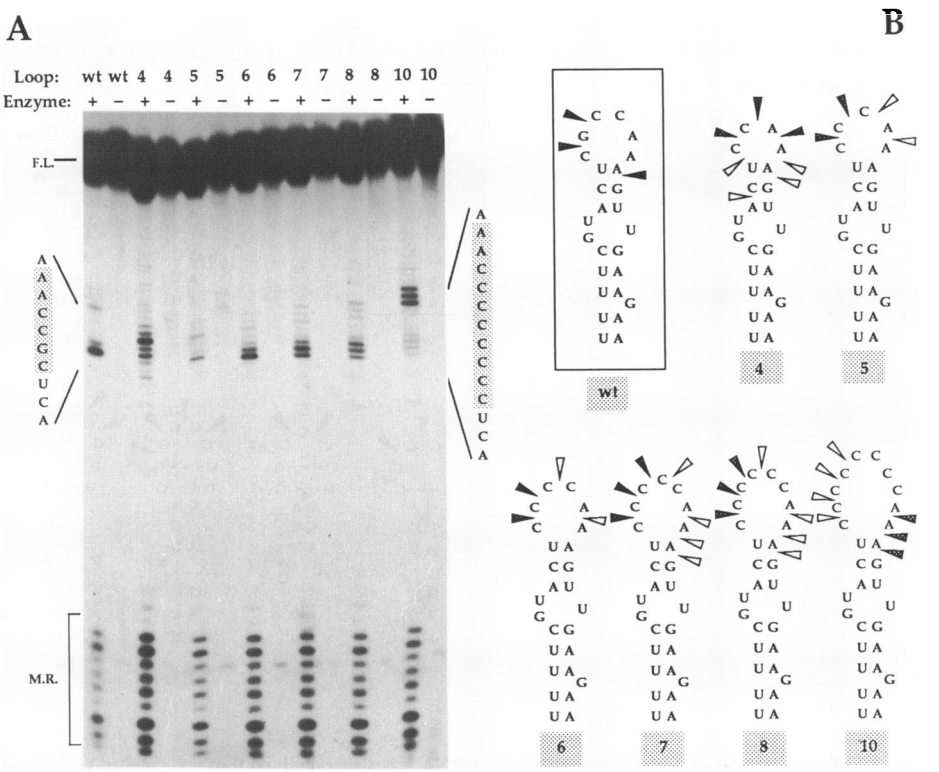

Figure 2. Partial ribonuclease T2 digests of ^{32}P- 5′-end labelled CopA RNA. CopA RNA was synthesized, purified and digested as described in Materials and Methods. Figure 2A shows an autoradiogram of such an analysis. The denotations wt, 4 through 10 refer to the expected loop sizes of the CopAs analyzed. (+) and (−) indicates incubation in the presence or absence of the ribonuclease. F.L and M.R. indicate the position of full-length, undigested CopA RNA and cleavages within the middle region of CopA, respectively [see Figure 1A, and (16)]. The primary loop II sequences for the wild-type and for the largest mutant loop are shown alongside the loop-specific cleavages in the autoradiogram. Loop nucleotides are shaded. Figure 2B shows a summary of the observed cleavages within the upper stem-loop II region of the RNAs. Filled and open arrowheads indicate major and minor cuts, respectively.

II of CopA, resulting in predicted loop sizes of 4−10 of the CopA recognition loops. Since the rather extensive changes in the CopA/CopT sequences might alter the overall folding of the RNAs, we used RNases to analyze the secondary structures of the *in vitro* transcribed, purified RNAs in solution.

Figures 2 and 3 show the results of such analyses performed with 5′-end-labelled CopA and CopT RNAs, respectively. Wild-type and mutant CopA RNAs were partially digested with RNase T2, such that on average << one cut/molecule was introduced (Figure 2A). The degree of cleavage can be estimated from the series of cuts within the middle region between stem-loops I and II of CopA (see Figures 1A and 2A: M.R.). RNase T2 is a single-strand-specific endonuclease that has a slight preference for A residues. The cleavage patterns in the loop II region and the upper stem of the CopA species are summarized in Figure 2B. The data indicate that the mutations did not introduce any gross alteration of the CopA structure, but changed the loop sizes approximately as predicted. The cleavage pattern of the 2C mutant RNA (denoted 4 in Figure 2) may suggest some 'breathing' of the upper, three base-pair stem. Likewise, in the largest loop (Figure 2: 10/mutant 8C), increased cleavages at the A residues indicate partially single-stranded character of the upper stem.

The analysis of CopT RNAs was performed similarly, but RNase T1 was used. The enzyme cleaves 3′ of G residues that are not involved in base-pairing. This probes for the accessibility of the G's within the CopT loop II sequence. Figure 3A shows such an analysis, and a summary of the cleavage data is presented in Figure 3B. The results indicate that the insertion of G's increased the sizes of the loop. However, RNAs with mutations 4C−8C (denoted 6−10 in Figure 3A) show weaker cleavages after the 3′-most G residues, which suggests the formation of additional G:U base pairs extending the short upper helix. This presumably reduces the actual loop sizes of CopT variants wt, 6, 7, 8, and 10 (Figure 3) to approximately 4, 4, 3, 4, and 6 nucleotides, respectively. A further observation relevant to the *repA-lacZ* fusion experiments described below is that all CopT RNAs show identical cleavage patterns outside the stem-loop II region, indicating that no major folding changes were induced by the mutations. An exception is mutant 6C (8 in Figure 3), which showed cleavage at a G residue not accessible to the RNase in the other CopT RNAs. This G is located at position 164 in the CopT sequence (27), and is complementary to a C residue on the 5′-side of the CopA stem-loop I. The implications of this local secondary structure change are not clear.

In vitro binding rates of CopA and CopT RNAs with altered sizes of loop II

Previous work has shown that the binding rates of pairs of CopA/CopT RNAs can be measured accurately *in vitro*. In the cases studied so far, changes in the binding rate constants of mutant RNAs and wild-type RNAs faithfully reflected the change in plasmid copy numbers of plasmids carrying wild-type or mutant *copA/copT* sequences (6, 7, 8; and unpublished data).

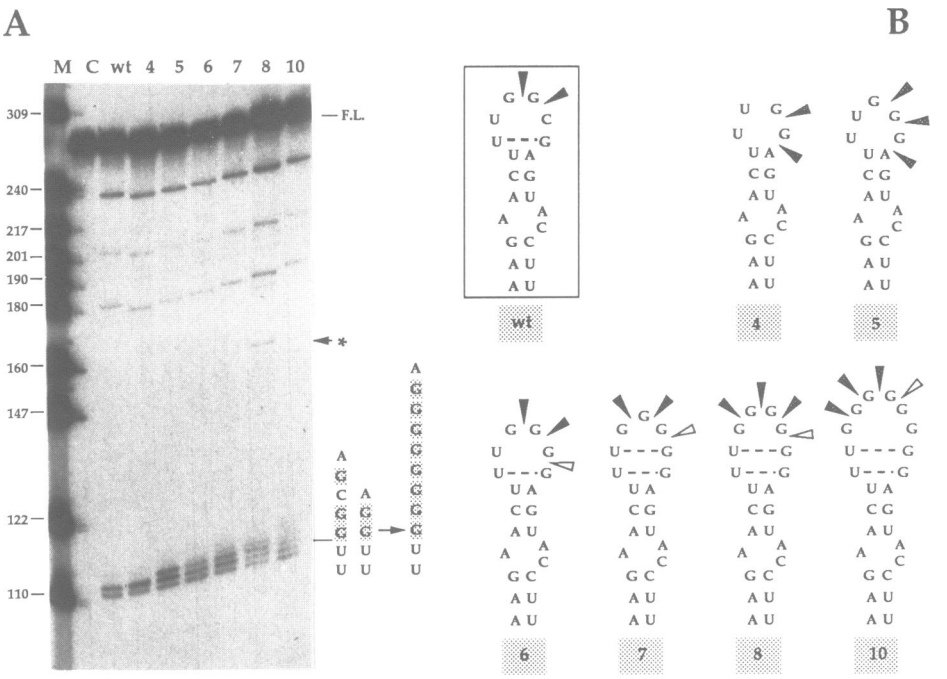

Figure 3. Partial ribonuclease T1 digests of ^{32}P- 5'-end labelled CopT RNA. CopT RNA was synthesized, purified and digested as described in Materials and Methods. The denotations wt, 4 through 10 refer to the expected loop sizes of the CopTs analyzed. M: size marker ([^{32}P]-end-labelled *Msp*I-fragments of pBR322). The sizes of the fragments are indicated on the left. C: control incubation in the absence of enzyme. F.L: full length CopT RNA. An extra band appearing in the analysis of mutant '8' (mutation 6C) is indicated by an asterisk and corresponds to a cleavage after a G at position 164 in the RepA mRNA (see Results). The primary loop II sequences for wild-type, the smallest and the largest mutants, respectively, are indicated next to the corresponding loop-specific cleavages in the autoradiogram. G residues in the presumed loops are emphasized by shaded letters. Figure 3B shows a summary of the observed cleavages within the upper stem-loop II region of the RNAs. Filled and open arrowheads indicate major and minor cuts, respectively. Dashed lines indicate G-U base-pairs proposed on the basis of the cleavage patterns.

This means that if, due to a *copA/copT* mutation, the binding rate constant (called k_{app}) is decreased three-fold, the copy number of the mutant plasmid increases approximately three-fold compared to that of a wild-type plasmid. Furthermore, the binding pathway was shown to initiate by the formation of a transient intermediate where loop II sequences of CopA and CopT interact (7). This step was found to be rate-limiting for the overall binding reaction, ultimately resulting in the full RNA duplex (8).

In order to investigate whether changes in the size of the CopA/CopT loops involved in the primary binding step would affect binding rates between CopA and CopT, we determined k_{app} for the homologous pairs of wild-type and mutant CopA/CopT RNAs (Materials and Methods; 6). The highest k_{app} value was determined for the wild-type RNA pair (Table 2). The binding rate constant measured for the mutant pair with a wild-type size loop II (6nt) was decreased about three-fold. A decrease in binding rate of this mutant RNA pair is expected, since the nucleotide change leads to a higher $\Delta G°$ for the complementary loop sequences according to the Tinoco rules (38). The highest k_{app} values of mutant CopA/CopT RNA pairs were obtained for mutants 5−7, and the lowest ones for those with the smallest and largest loop sizes. This indicates that CopAs with small (4 nt) as well as large (10 nt) loop II's have significantly decreased binding rates, not only compared to the wild-type RNA pair ($\approx$13-fold and $\approx$160-fold lower, respectively), but, more importantly, also compared to the CopA/CopTs with intermediate loop sizes ($\approx$5-fold and $\approx$50-fold lower, respectively). The data suggest that there is an optimum loop size for obtaining the highest binding rates.

Since the most extreme loop size mutants showed large decreases in the binding rates, we had to consider the possibility that the binding pathway was altered in these mutants. This was previously observed for a truncated CopA RNA species, CopI (8), where, instead of the formation of the 'kissing complex', the nucleation of complete RNA duplex formation had become rate-limiting. Loop-loop interaction precedes the nucleation of RNA duplex formation within the single-stranded stretch of nucleotides between stem-loops I and II of CopA RNA (7). This latter step is intramolecular and therefore concentration-independent. In contrast, if 'kissing complex' formation is the rate-limiting step, the binding rates should change as a function of the concentrations of the reactant RNAs. Therefore, we tested binding of all RNA pairs at varying RNA concentrations. All pairs showed the expected linear increase in binding rate when we raised the concentration of the RNA present in high molar excess (up to 3×10^{-7} M; data not shown). This indicates that no change of rate-limiting step has taken place in the mutant CopA/CopT binding pathway, and that the measured overall binding rate constants mainly or exclusively reflect the rate of formation of the 'kissing intermediate' (8).

Relative plasmid copy numbers of loop size mutant plasmids

A direct test for the effect of *copA/copT* mutations on the properties of the replication control circuit is to measure the copy numbers of mini-R1 plasmids carrying the mutations in question. We used the pMB1-R1 hybrid plasmids of the pGW64-series (Table 1). When these hybrid replicons are transformed into a *polA* background, only the R1 replicon is functional, and its

Table 2. Effect of loop size mutations on binding rate constants between CopA and CopT RNA *in vitro*, on relative plasmid copy number, and on *repA-lacZ* expression *in vivo*.

CopA loop II sequence	[a] k_{app} ($M^{-1}s^{-1}$)	[b] expected activity factor (EAF)	[c] relative copy number	[d] relative β-Gal. activity
w.t. (CGCCAA)	1.320×10^6	1.0	1.0	1.0
4 (C_2AA)	0.100×10^6	13.2	10.3	4.4
5 (C_3AA)	0.307×10^6	4.3	7.5	3.3
6 (C_4AA)	0.423×10^6	3.1	3.7	1.6
7 (C_5AA)	0.571×10^6	2.3	3.7	1.7
8 (C_6AA)	0.243×10^6	5.4	4.0	1.0
10 (C_8AA)	0.008×10^6	165.0	7.5	1.0

[a] The *in vitro* binding assays were performed as described in Materials and Methods. k_{app} was determined as in (6). The values shown are averages of three independent determinations.

[b] The expected activity factor (EAF) describes the relative expected increase in CopA-controlled *repA* expression or plasmid copy number due to the change in k_{app}. Since inhibition by CopA is correlated to k_{app}, and *repA* expression is correlated to $1/k_{app}$, the EAF of the mutants is expressed as ($1/k_{app}$-mutant)/($1/k_{app}$-w.t.). For the wild type, this factor becomes 1.0.

[c] Single cell resistance (SCR)-tests were performed as described (Materials and Methods). The plasmids used were pGW64 (w.t.) and pGW64-2C through pGW64-8C (mutants, see Materials and Methods). The values shown are averages of three independent experiments. The resistance level conferred by the wild-type plasmid (pGW41) was set to unity, and the resistance levels of cells carrying the mutant derivatives were expressed relative to the wild-type plasmid.

[d] RepA-LacZ protein synthesis *in vivo* was assayed as described (25). The plasmids used for this test were pGW177-L (w.t.) and pGW177-2C-L through pGW177-8C-L (mutants, see Materials and Methods). The values shown are averages of six independent experiments. They are represented as relative β-galactosidase activities (wild-type fusion plasmid is set to 1.0).

relative copy number can be determined by using a single cell resistance test (SCR) (24; Materials and Methods). Table 2 shows the result of such a test performed on wild-type and mutant plasmids. Plasmids carrying the various loop size mutations had elevated copy numbers compared to the wild-type plasmid. Most importantly, the relative copy number increases of the mutant plasmids appear to be approximately correlated to the $1/k_{app}$-values in Table 2 (cf. columns three and four in Table 2), with the exception of plasmid pGW41-8C (see Discussion). This indicates that the copy number changes were predominantly or exclusively due to the changes in binding rate constants between CopA and CopT.

Effects of loop-size mutations on repA-lacZ expression *in vivo*

The effect of mutant and wild-type CopA/CopT duplex formation can also be determined by measuring the *in vivo* synthesis of RepA-LacZ fusion protein encoded by plasmids carrying translational fusions under the control of the *copA/copT* system (14, 15, 18, 20, 25, 28). High rates of duplex formation generally result in low *repA-lacZ* expression and *vice versa*.

We constructed mutant derivatives of the translational *repA-lacZ* fusion plasmid pGW177-L (Table 1). The β-galactosidase activities of cells carrying mutant or wild-type plasmids were determined (Table 2, column five). The *repA-lacZ* expression of cells harboring mutant plasmids was elevated compared to the activities measured in cells carrying the wild-type construct, which reflects the lower k_{app}-values obtained for the mutant RNAs in the binding assay, although the correlation was less clear than for the copy number measurements. For the mutant plasmids with the two largest loop sizes, *repA-lacZ* expression was unexpectedly low (see Discussion).

Analysis of steady-state CopA and CopT RNA in plasmid-carrying cells

The loop size mutations introduced rather severe changes into CopA and CopT RNAs, both in terms of primary sequence and structure of the loop region. Therefore, quantitative deviations of the results obtained *in vivo* (SCR-test/*repA-lacZ* expression, Table 2) from the results of the *in vitro* binding assay (Table 2) could be due to effects on metabolic stability, transcriptional pausing pattern or alternative folding pathways of the RNAs involved. Folding pathways and secondary structure changes cannot be easily analyzed *in vivo*. However, Northern analysis on RNA extracted from plasmid-carrying cells can give

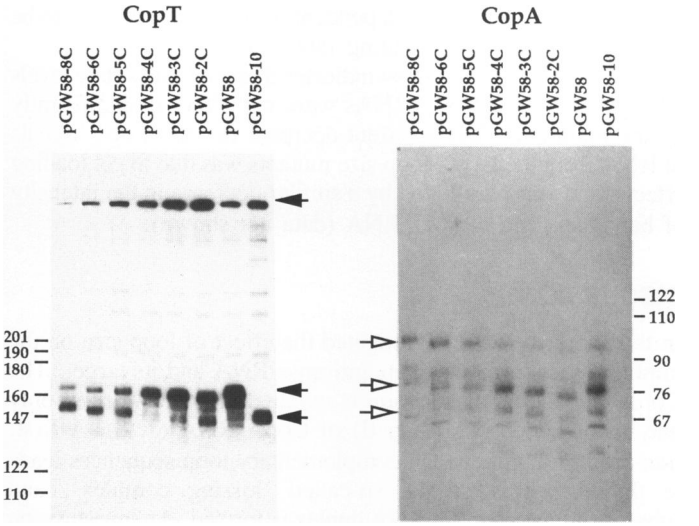

Figure 4. Northern blot analysis of CopT and CopA RNAs *in vivo*. Total RNA was extracted from cells carrying various plasmids of the pGW58-series and used for Northern blot analysis as described [Materials and Methods; (18)]. The left-hand panel shows the band pattern of CopT RNA, and the right-hand panel shows CopA-specific bands. The plasmids carried by the cells are indicated above the autoradiographs. The positions of some marker bands (end-labelled *Msp*I-fragments of pBR322) are shown for size comparisons. The three bands indicated by filled arrowheads show the positions of full-length CopT RNA (top), duplex-dependent RNase III-cleaved CopT (middle) and a CopT transcription pause band of ≈ 140 nt (bottom). Open arrowheads indicate the positions of full length CopA RNA (top), duplex-dependent RNase III-cleaved CopA (middle) and RNase E-cleaved CopA (bottom). The identity and origin of both the CopA- and CopT-specific bands has been discussed in detail previously (18). Note that no CopA RNA is produced in cells carrying plasmid pGW58-10 (Table 1), and consequently, RNase III does not cleave CopT (see lanes pGW58-10).

information on the relative abundance of CopA and CopT RNAs. In addition, binding of CopA and CopT results in an RNA duplex which is rapidly and specifically cleaved by the host enzyme RNase III, which provides a qualitative test for CopA/CopT binding (18). We performed Northern analyses on RNA preparations from cells carrying mutant and wild-type plasmids (Materials and Methods). As shown in Figure 4, the band patterns of wild-type and mutant plasmid RNAs are qualitatively identical. The relative intensities of some characteristic bands are altered, which can be explained by differences in antisense-target RNA binding. Thus, lower binding rates lead to a decrease in CopA/CopT duplex formation, which results in lower intensities of CopA and CopT-specific bands that are due to duplex-dependent RNase III cleavages [see Figure 4, and (18) for a detailed analysis of the band patterns]. E.g., *in vitro*, wild-type CopA/CopT duplexes are formed more rapidly than CopA/CopT duplexes of mutant 2C (Table 1), and faster RNA duplex formation *in vivo* is indicated by the higher relative intensity of the bands representing the duplex-dependent RNase III cleavage products (Figure 4: middle arrowheads) over the duplex-independent bands—corresponding to full-length, terminated transcript and a transcriptional pause RNA, respectively (Figure 4: upper and lower arrowheads). Again, mutant 8C is abberant, since the duplex-dependent bands were expected to be weaker due to a lower binding rate constant.

The Northern analysis also indicates that the steady state levels of both CopA and CopT RNAs were not affected significantly by the mutations. The apparent decrease of total CopT signals of RNA from the larger loop size mutants was due to gel loading effects, and was parallelled by a similar decrease in the intensity of bands specific for M1 RNA (data not shown).

DISCUSSION

In this work we have investigated the effect of loop size on the binding reaction between an antisense RNA and its target. The CopA/CopT binding reaction is initiated at nucleotides in only one of the two loops (loop II) of CopA RNA (7, 8). A first, transient binding between complementary loop sequences leads to the formation of the so-called 'kissing complex', and subsequently a complete RNA duplex is formed. An investigation of the CopA/CopT system of R1 has shown that the rate-limiting step in the reaction pathway is the formation of the 'kissing complex' (7, 8). Only loop II appears to be involved in this step, and it was therefore feasible to ask whether the size of the loop affects the activity of the antisense RNA. Previous observations indicated that, in addition to the primary sequence of the loop nucleotides, loop structure and/or loop size might affect binding rates. Hence, we created a series of loop size mutations by varying the length of a series of C residues in CopA loop II (concomitantly resulting in a corresponding number of G residues in CopT), and tested their effect on CopA/CopT binding rates *in vitro* as well as CopA's inhibitory activity *in vivo*.

The binding rate constants (k_{app}) for the homologous pairs of mutant CopA and CopT RNAs showed a maximum for the loops designated 5–7 (mutants 3C–5C; Table 2). Smaller and larger loops bound at lower rates, in agreement with previous results on two high copy number R1 mutant plasmids (15, and unpublished). Note, however, that CopT loop sizes may be smaller than their CopA counterparts due to the formation of extra G-U pairs. This is already apparent for the wild-type pair, so that a 6-nucleotide loop has to bind to a (presumed) 4-nucleotide loop. The binding pathway of mutant CopA and CopT appears to be the same as that of the wild-type species, since for all RNA pairs the binding rates were linearly correlated with the concentrations of the RNAs in excess. This indicates that the formation of the 'kissing complex' is still rate-limiting, and that the mutations, at least primarily, affect this step.

The *in vivo* effects of RNA duplex formation were tested in two ways. Relative copy number determinations of mutant plasmids (Table 2) agreed reasonably well with the *in vitro* measurements, in that the inverse of k_{app} was correlated with relative copy number. *In vitro* and *in vivo* results deviated, however, when the larger loop size mutants were analyzed. Thus, the *in vitro* binding rate constant of CopA-8C to its homologous target RNA was drastically decreased compared to the mutant CopA/CopT pair with wild-type loop size ($\approx$50-fold; Table 2), whereas the copy number difference between the plasmids carrying these mutations, pGW41-8C and pGW41-4C, was only a factor of two (Table 2). The deviation of the *in vitro* from *in vivo* results is even more severe when binding rate constants are compared to *repA-lacZ* expression (Table 2). Here, both *repA-lacZ* fusion constructs carrying mutations 6C and 8C (designated 8 and 10 in Figures 2 and 3) show the lowest β-galactosidase activities. These values are as low as the ones of the wild-type fusion. We have no clear explanation for the abberant behaviour of, in particular, the largest loop mutant. The most likely possibilities, effects on transcriptional pausing within the run of G's in the CopT loop II sequence, or an adverse effect on CopA RNA half-life, were not supported by Northern analysis (Figure 4). We noted, however, that mutation 6C appeared to cause a local change in the secondary structure of CopT RNA, distal to the site of the mutation (Figure 3A). It is possible that a change in RNA folding affects the translational activity of the RepA mRNA. The greatest discrepancy between RNA binding rates and *in vivo* performance of the mutant plasmid was observed for mutant 8C, which was low both in *repA-lacZ* expression and relative plasmid copy number (Table 2). Since the RNAs of this mutant carry unusually long stretches of identical nucleotides, it may not be surprising that unexpected effects are seen *in vivo*. In particular, homopolymers of G residues (the CopT loop sequence contains 8 consecutive G's) have shown a tendency to aggregate (29). Alternatively, since the sequence around the *tap* Shine–Dalgarno (14) is GGGGAG, it may be possible for a CopA RNA with a large C-rich loop to bind directly to this sequence and to prevent *tap* translation. If this occurred, a direct inhibition of *tap* (and, thereby, *repA*) translation would, in part, compensate for the lower binding rate between the mutant CopA and its target.

The result that alterations of loop size have pronounced effects on binding rates between CopA and CopT RNAs raises the question of how to interprete this finding. The two complementary loop sequences of CopA and CopT RNA transiently form a short RNA helix which involves 6–8 base pairs (7). The subsequent step of RNA duplex formation is fast, and its rate is not limiting for the overall reaction (8). The loop size mutations studied in this communication, as well as the previously characterized base change mutations in several IncFII-plasmids (see references in [4]) appear to decrease the rate of formation of the 'kissing intermediate'. We showed recently that differences in binding strength between loop II sequences in mutant and wild-type CopA and CopT RNAs alone cannot account for the observed

differences in plasmid copy number (6, 8). Thus, base changes leading to a predicted increase in the K_D of a CopA/CopT loop from a wild-type to a mutant by a factor of 90 only result in an approximately three-fold higher copy number (6, 8). The low binding rate constants measured for mutants 6C and 8C (Table 2) agree with the above conclusion. If equilibrium binding constants between accessible, single-stranded loop nucleotides were determining overall binding rates, k_{app} values should increase as the number of loop nucleotides increases. Since this is not supported by the data presented, the mutations must primarily alter the association rate constant that characterizes loop-loop helix formation (8). Thus, high binding rates appear to require a proper structure that presents the nucleotides that are involved in the primary recognition step (i.e., loop II in CopA). The three-dimensional structure of the loop nucleotides is probably also affected by nucleotides within the three base-pairs in the upper stem region (Figure 1A). This is expected in part from stacking effects, but also because a short unstable helix of 2−3 base pairs, which initially forms between complementary CopA and CopT loop nucleotides, is extended to the 6−8 base pair helix of the intermediate (7). This extended helix has been shown to involve bases in the upper stem region, and requires therefore an disruption of these three base pairs. From the results presented, we cannot define an optimal loop structure. Thus, it will be of interest to obtain detailed information on the structure of the loop regions of a more extensive collection of fast and slow binding CopA and CopT RNA species.

The structural requirements for the recognition process that determine overall binding rates of antisense/target RNA binding reactions may be similar or different from features that determine the activities of other RNAs. Similar to the recognition reaction of CopA/CopT, a tRNA has to bind to specific codons within a mRNA during translation. All tRNAs have anticodon loops of 7 nuclotides, and their geometry appears to present the particular set of three nucleotides, the anticodon, for interaction with the codon in the mRNA, rather than permitting *any* of the loop nucleotides to find complementary nucleotides for base-pairing (30, 31). Thus, loop sizes of 7, as in tRNA, in RNAI of plasmid ColE1 (three 7-nt loops; [32]) and in RNA-OUT of *Tn*10 (1), and loop sizes of 6, as in CopA RNA (16), may be preferred for highly specific and rapid recognition of a target sequence. Hairpin loops of 4 nucleotides, in contrast, are the preferred stem-loops in rRNAs (33). Tetranucleotide loops, in particular the ones conforming to the UNCG or GNRA motifs (34), are extraordinarily stable. Recent data suggest that stem-loops with a loop size of 4 or 5 have the highest degree of stability, independent of the sequence of the loop nucleotides (35). Thus, these small loops may be preferred since they could serve as nucleation sites in proper folding of larger RNAs (36). In natural antisense RNAs, tetranucleotide loops are rarely found (1), and their efficiencies have not been tested.

In summary, loop stability appears to be of minor importance for the efficiency of antisense RNAs. Likewise, extended single-stranded sequences within RNAs and large loops are not favorable for obtaining high binding rates between antisense RNAs and their targets (see Results; F. Söderbom, unpublished). We propose that the three-dimensional structure of the hairpin loop that initiates the binding reaction has to be optimally presented in order to proceed rapidly from the first, reversible formation of a small number of base pairs to the more stable 'kissing intermediate'. In the CopA/CopT system, this step may additionally be affected by the presence of bulges within the upper stem region.

The results obtained during the investigations of some well-characterized, natural antisense RNA systems (1, 5, 6, 8, 11), can be used for guidance in the design of efficient artificial antisense RNA control systems. We can conclude that the rate of duplex formation between antisense and target RNA is a major factor in determining the efficiency of antisense RNA control. The importance of the characteristic stem-loop structures, and of the loop nucleotides, in antisense and target RNAs has been recognized previously. Here, we show that also loop sizes affect RNA binding rates. Howevere, the complexity of the results presented above also indicates the problem of dealing with unsuspected side-effects when designing artificial antisense RNA genes. Thus, secondary structures of RNAs in solution (and most certainly also *in vivo*) may deviate from the predicted ones, and potential secondary sites of interactions between antisense and target RNAs can alter antisense RNA control in unpredicted ways. Further work will be required to study the relationship between loop sizes and the particular structural details that favor rapid binding.

ACKNOWLEDGEMENTS

The technical assistance of Solveig Andersson is gratefully acknowledged. We thank L.Kirsebom for synthesis of deoxyoligoribonucleotides. We are grateful to K.Nordström, F.Söderbom and D.Andersson for critical reading of the manuscript. This work was supported by The Swedish Natural Science Research Council (E.G.H. Wagner and K.Nordström), the Swedish Board for Technical Development (E.G.H.Wagner), and the Swedish Cancer Society (K. Nordström).

REFERENCES

1. Simons, R.W. and Kleckner, N. (1988) *Annu. Rev. Genet.* **22**, 567−600.
2. Kimelman, D. and Kirschner, M.W. (1989) *Cell* **59**, 687−696.
3. Hildebrandt, M. and Nellen, W. (1992) *Cell* **69**, 197−204.
4. Nordström, K., Molin, S. and Light, J. (1984) *Plasmid* **12**, 71−90.
5. Polisky, B. (1988) *Cell* **55**, 929−932.
6. Persson, C., Wagner, E.G.H. and Nordström, K. (1988) *EMBO J.* **7**, 3279−3288.
7. Persson, C., Wagner, E.G.H. and Nordström, K. (1990a) *EMBO J.* **9**, 3767−3775.
8. Persson, C., Wagner, E.G.H. and Nordström, K. (1990b) *EMBO J.* **9**, 3777−3785.
9. Tomizawa, J. (1984) *Cell* **38**, 861−870.
10. Tomizawa, J. (1985) *Cell* **40**, 527−535.
11. Tomizawa, J. (1990) *J. Mol. Biol.* 212, 683−694.
12. Lacatena, R.M. and Cesarini, G. (1983) *J. Mol. Biol.* 170, 635−650.
13. Kittle, J.D., Simons, R.W., Lee, J. and Kleckner, N. (1989) *J.Mol.Biol.* **210**, 561−572.
14. Blomberg, P., Nordström, K., and Wagner, E.G.H. (1992) *EMBO J.* **11**, 2675−2683.
15. Givskov, M. and Molin, S. (1984) *Molec. Gen. Genet.* **194**, 286−292.
16. Wagner, E.G.H., and Nordström, K. (1986) *Nucleic Acids Res.* **14**, 2523−2538.
17. Casadaban, M.J. and Cohen, S.N. (1980) *J. Mol. Biol.* **138**, 179−207.
18. Blomberg, P., Wagner, E.G.H. and Nordström, K. (1990) *EMBO J.* **9**, 2331−2340.
19. Larsen, J.E.L., Gerdes, K., Light, J. and Molin, S. (1984) *Gene* **28**, 45−54.
20. Öhman, M. and Wagner, E.G.H. (1991) *Molec. Gen. Genet.* 230, 321−328.
21. Sambrook, J., Fritsch, E.F., and Maniatis, T. (1989) Molecular Cloning: A Laboratory Manual. Cold Spring Harbor Laboratory Press, Cold Spring Harbor.
22. Taylor, J.W., Schmidt, W., Cosstick, R., Okruszek, A. and Eckstein, F. (1985) *Nucleic Acids Res.* **13**, 8749−8764.

23. Taylor, J.W., Ott, J. and Eckstein, F. (1985) *Nucleic Acid Res.* **13**, 8765–8785.
24. Uhlin, B.E., and Nordström, K. (1977) *Plasmid* 1, 1–7.
25. Berzal-Herranz, A., Wagner, E.G.H., Díaz-Orejas, R. (1991) *Mol. Microbiol.* 5, 97–107.
26. Milligan, J.F., Groebe, D.R., Witkerell, G.W., and Uhlenbeck, O.C. (1987) *Nucleic Acid Res.* 15, 8783–8798.
27. Öhman, M. and Wagner, E.G.H. (1989) *Nucleic Acids Res.* 17, 2557–2579.
28. Wagner, E.G.H., Blomberg, P. and Nordström, K. (1992) *EMBO J.* **11**, 1195–1203.
29. Jaskunas, S.R., Cantor, C.R., and Tinoco, Jr., I (1968) *Biochemistry* 7, 3164–3178.
30. Fuller, W. and Hodgson, A. (1967) *Nature* **215**, 817–821.
31. Grosjean, H., Söll, D.G. and Crothers, D.M. (1976) *J. Mol. Biol.* **103**, 499–519.
32. Tamm, J. and Polisky, B. (1983) *Nucleic Acids Res.* **11**, 6381–6397.
33. Woese, C.R., Winker, S. and Gutell, R.R. (1990) *Proc. Natl. Acad. Sci. USA* **87**, 8467–8471.
34. Antao, V.P., Lai, S.Y. and Tinoco, Jr., I (1991) *Nucleic Acids Res.* **19**, 5901–5905.
35. Groebe, D.R. and Uhlenbeck, O.U. (1988) *Nucleic Acids Res.* **16**, 11725–11735.
36. Heus, H.A. and Pardi, A. (1991) *Science* **253**, 191–194.
37. Ryder, T.B., Davison, D.B., Rosen, J.I., Ohtsubo, H. and Ohtsubo, E. (1982) *Gene* **17**, 299–310.
38. Tinoco, I., Jr., Borer, P., Dengler, B., Levine, M.D., Uhlenbeck, O.C., Crothers, D.M. and Gralla, J. (1973) *Nature*, **246**, 40–41.